


Tug-of-War between Internal and External Frictions and Viscosity Dependence of Rate in Biological Reactions

Saumyak Mukherjee¹, Sayantan Mondal¹, Subhajit Acharya, and Biman Bagchi^{1*}
Solid State and Structural Chemistry Unit, Indian Institute of Science, Bengaluru 560012, Karnataka, India

 (Received 21 July 2021; revised 13 December 2021; accepted 11 February 2022; published 7 March 2022)

The role of water in biological processes is studied in three reactions, namely, the Fe-CO bond rupture in myoglobin, GB1 unfolding, and insulin dimer dissociation. We compute both internal and external components of friction on relevant reaction coordinates. In all of the three cases, the cross-correlation between forces from protein and water is found to be large and negative that serves to reduce the total friction significantly, increase the calculated reaction rate, and weaken solvent viscosity dependence. The computed force spectrum reveals bimodal $1/f$ noise, suggesting the use of a non-Markovian rate theory.

DOI: 10.1103/PhysRevLett.128.108101

Despite the importance of water in biological activities [1–3], our understanding of the microscopic manner by which water influences biological processes remains vague. Complex biochemical reactions such as folding, dissociation, aggregation, and fibrillation of proteins are deeply influenced by both water and protein motions [4–7]. Frauenfelder *et al.* suggested that the motions of proteins are “slaved” to the dynamics of water [8,9]. This slaving mechanism could be mediated by a flow of energy between protein and water, largely modulated by the side-chain fluctuations and low dielectric constant of the protein core [10]. Such processes require characterization by multidimensional free energy landscapes [11–13]. The ruggedness of such free energy landscapes are overcome by internal protein fluctuations [14,15]. Best and co-workers suggested that friction from internal protein motions dominate the frictional resistance on such processes [4,5,15]. Several studies have observed a weak viscosity dependence of the rate of these processes [9,16–19], which has been rationalized in terms of protein internal friction. Makarov and co-workers studied internal friction in terms of the average reconfiguration timescales of disordered and unfolded proteins and their relations to solvent viscosity [18,20]. The low dielectric constant of the protein interior [21] allows the long-range electrostatic forces from water to influence even the protein core [10].

In the present work, we study this coupling in three separate proteins, namely, myoglobin, GB1, and insulin dimer. A reaction coordinate is essential to understand the energy landscape of a chemical process. We use the formalism (and also the notation) of Oxtoby and others in the context of vibrational energy relaxation [22–25] where one expands the potential energy as a function of the bond reaction coordinate, denoted by Q [Eq. (1)].

$$V(Q) = V(Q=0) + \left(\frac{\partial V}{\partial Q}\right)Q|_{Q=0} + \frac{1}{2} \left(\frac{\partial^2 V}{\partial Q^2}\right)Q^2|_{Q=0}. \quad (1)$$

The reaction coordinate in the present study is also a bond vector. In each of the three proteins, we focus on one or more bonds (coordinate or hydrogen bonds) that need to break for the proteins’ biological purposes. Thus, an appropriate reaction coordinate is the bond length. The specification of a bond requires positions of two atoms in the three dimensional coordinate space where these bonds are represented by vectors. For example, in myoglobin, the bond is between the Fe and CO groups in the protein [Fig. 1(a)]. \mathbf{Q} , in this case is defined as a vector as in Eq. (2).

$$\mathbf{Q} = \mathbf{B}_{\text{Fe-CO}} = \mathbf{r}_{\text{Fe}} - \mathbf{r}_{\text{CO}}, \quad (2)$$

where, \mathbf{r}_{Fe} and \mathbf{r}_{CO} refer to the positions of the Fe and the CO groups, respectively. However, the scenario is different in cases of GB1 [Fig. 1(b)] and insulin dimer [Fig. 1(c)]. In these cases, the interactions of concern are four hydrogen bonds, the rupture of which are crucial for unfolding [26–29] or dissociation [30–35] of the protein. The reaction coordinate is defined by a sum over all the four bond vectors (\mathbf{B}_i , $i = 1, 4$) as in Eq. (3).

$$\mathbf{Q} = \sum_{i=1}^4 \mathbf{B}_i = \sum_{i=1}^4 (\mathbf{r}_{D_i} - \mathbf{r}_{A_i}). \quad (3)$$

Here, D and A represent the hydrogen bond (HB) donor and acceptor, respectively. To drive the dissociation process, the individual forces acting on the two atoms (or groups of atoms) that constitute the bonds must be oppositely directed.

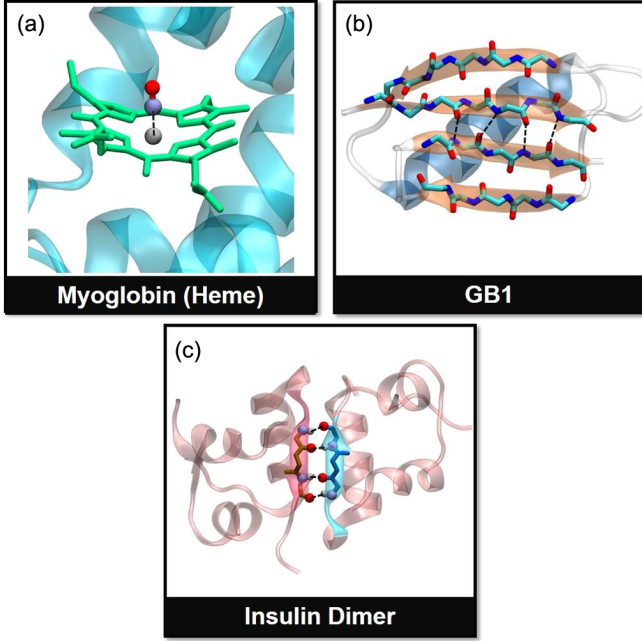


FIG. 1. Pictorial description of the reaction coordinates in the three systems studied in this work. (a) Fe-CO bond in the heme unit of myoglobin, (b) hydrogen bonds (HBs) between parallel β sheets in GB1, and (c) the junction HBs in insulin dimer. These bonds vectors act as the reaction coordinates (black dashed lines) in this study.

The motion of the bond is described by a generalized Langevin equation [36] for the reaction coordinate \mathbf{Q} .

$$\mu\ddot{\mathbf{Q}}(t) = \mathbf{F}(\mathbf{Q}) - \int_0^t d\tau \zeta(\tau) \dot{\mathbf{Q}}(t-\tau) + \mathbf{R}(t) \quad (4)$$

where μ is the effective mass along the reaction coordinate and $\mathbf{F}(\mathbf{Q})$ is the systematic force due to bonding. The time dependent friction ($\zeta(t)$) is related to the fluctuating force $\mathbf{F}(t)$ through the fluctuation-dissipation theorem [37].

$$\langle \mathbf{R}(0) \cdot \mathbf{R}(t) \rangle = 2dk_B T \zeta(t). \quad (5)$$

Here, d defines the dimensionality of the system. Thus, the friction can be obtained from the force-force time correlation function. We calculate the forces experienced by these atoms and add them (with the appropriate sign reversal) to obtain the total force vector on the concerned bonds which are held fixed. We next calculate the auto-correlation function of the force fluctuations and use the Kirkwood formula [38,39] to obtain the friction. We execute this exercise separately for the effects of protein and water on the bonds, which allows us to segregate the contributions from these two domains and their cross-correlation. Accordingly, the total friction experienced by these bonds contains three contributions.

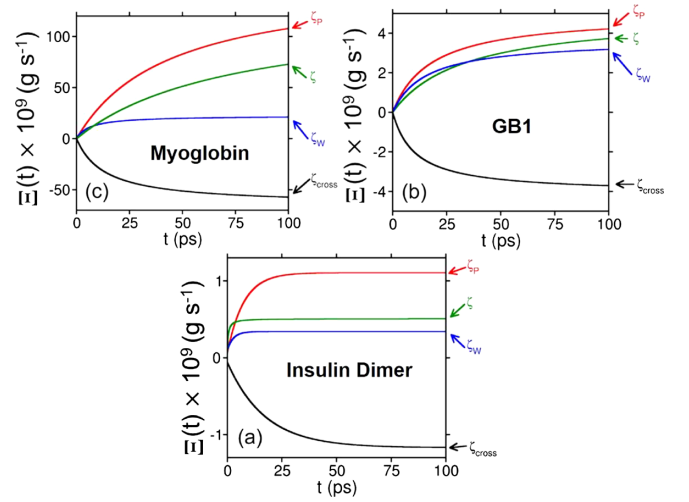


FIG. 2. Time evolution of the auxiliary function $\Xi(t)$ for different contributions to the total friction experienced by (a) Fe-CO bond in the heme unit of myoglobin, (b) HBs between parallel β sheets in GB1, and (c) the junction HBs in insulin dimer. Color code: red, contributions from protein; blue, from water; and black, the cross term. The total response is represented by the green color. The cross term contributes a huge negative value, which brings down the value of total friction.

$$\zeta = \zeta_P + \zeta_W + \zeta_{cross}. \quad (6)$$

In Eq. (6) the subscripts p and w refer to protein and water, respectively, while $cross$ represents the coupled term. The origin of the individual friction terms [Eq. (6)] can be realized by decomposing the total force (\mathbf{F}) into contributions from protein and water [40]. To compare these friction contributions individually, we introduce an auxiliary time-dependent function $\Xi(t)$ [Eq. (7)], which is an integral over the force autocorrelation function. In the limit $t \rightarrow \infty$, this reduces to the Kirkwood formula, which gives the value of friction.

$$\Xi(t) = \frac{1}{3k_B T} \int_0^t d\tau \langle \delta \mathbf{F}(0) \cdot \delta \mathbf{F}(\tau) \rangle, \quad (7)$$

$$\zeta = \lim_{t \rightarrow \infty} \Xi(t).$$

Here, k_B is the Boltzmann constant and T is the temperature of the system. A rigorous derivation of the Kirkwood formula follows from Zwanzig's projection operator technique [36,38]. The foremost requirement is that the space of the dynamical variable in question should not be coupled with the bath degrees of freedom. In the present case, it is accomplished by fixing the coordinate space positions of the bonds under investigation. This is a widely used technique [24,51].

In Fig. 2 we show the temporal evolution of $\Xi(t)$ for the contributions from protein internal friction (ζ_P) (red), water external friction (ζ_W) (blue), and the cross term (ζ_{cross}) (black), along with that of the total friction (ζ) (green).

TABLE I. Values of friction obtained from the Kirkwood formula for the three studied systems.

Contribution	$\zeta \times 10^9$ (g s ⁻¹)		
	Myoglobin	GB1	Insulin dimer
Protein	154.8	4.97	1.17
Water	22.0	3.66	0.34
Cross	-64.2	-4.09	-1.33
Total	112.6	4.54	0.18

For GB1 [Fig. 2(b)] and insulin dimer [Fig. 2(c)], the plots are averaged over the four concerned hydrogen bonds in each case. We obtain the zero-frequency friction by extending the upper limit of integration to infinity. The values thus obtained are given in Table I.

In all three cases, the protein internal friction contributes the major fraction. However, the total cross term is negative and comparable to the internal friction (particularly in insulin dimer and GB1). This results in a significant decrease in the total friction experienced by the relevant reaction coordinate. It is to be noted that the total cross-friction term is a summation of two individual cross terms [40]. Thus ζ_{cross} , that acts as a lubricant at these bonds, increases the rate of the dissociation reaction. This appears to be a general feature in all the systems.

To get an idea about the relaxation timescales, we must study the force autocorrelation functions (FACF) separately [40]. As discussed before, there are four terms (protein, water, and two of their cross-correlation terms) that contribute to the total force ACF. We separately compute these contributions [40]. For the cross-correlation, the relaxation is studied for the average of the two terms. Most of these time correlation functions are found to show multiexponential decay.

In insulin dimer and GB1 (for the forces on the relevant hydrogen bonds), the relaxation of protein FACF is slower than that of water. For the Fe-CO bond in myoglobin, however, the scenario is different. Here, the protein contribution of FACF shows an initial oscillatory decay, which is faster than that of water. This oscillatory behavior is translated into faster decay of the total FACF.

The value of the stretching frequency of the Fe-CO bond is ~ 1945 cm⁻¹ [52]. At room temperature, this frequency corresponds to a timescale of ~ 16 fs. This corroborates with the ultrafast solvation response observed by Fleming and co-workers (~ 20 fs) [53]. Hence, one can state that the ultrafast solvent polarization fluctuations couples with the Fe-CO bond vibration along with the vibrational modes of the protein. The present calculation does not explicitly take the quantum effects into account that might be important for Fe-CO coordination. Although the inclusion of quantum effects shall change the relative contributions, the trend should remain the same.

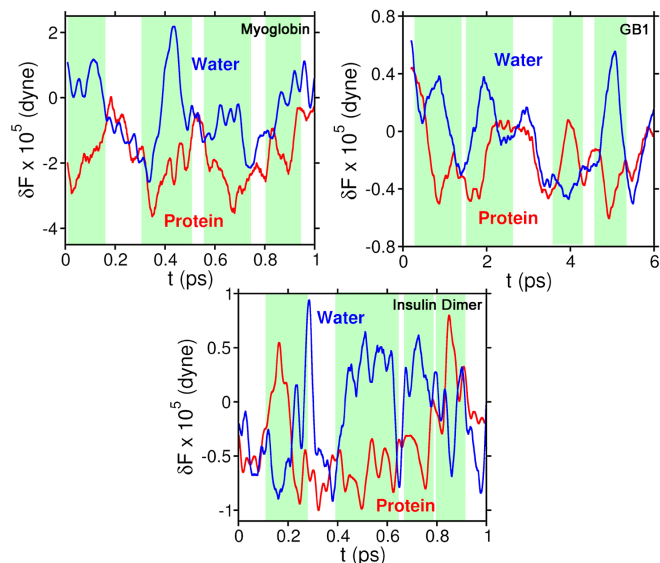


FIG. 3. Temporal evolution of the fluctuations in the magnitude of the force on the relevant reaction coordinates in myoglobin, GB1, and insulin dimer. The red color represents the force contribution from protein and the blue color represents that from water. These two contributions show pronounced anticorrelated fluctuations in all three proteins. One short-time trajectory for each of the systems is shown here. The green rectangles represent the anticorrelation events.

The order of magnitude of the timescale components varies from system to system. These are tabulated in [40]. The overall relaxation in GB1 is one order of magnitude slower than that of insulin dimer. In all the proteins, we observe a surprisingly dominant ultrafast component around ~ 100 fs in the protein component which is similar to the ultrafast solvation component well-known for water [54]. There are certain intermediate-to-high frequency normal modes in protein like internal hydrogen bonds, or dihedral angle fluctuations. These vibrations can combine to give rise to the ultrafast component [18,55]. But, they could also originate from the dynamical coupling with water fluctuations.

The cross-TCF shows triexponential decay. The amplitude of the cross-TCF is negative, as already mentioned. This accelerates the relaxation of total FACF. Such acceleration of dynamical relaxation by a negatively cross-correlated contribution has been previously reported in several other cases [54]. The negative cross-correlation function was extensively discussed in the context of ion diffusion [56–58].

The anticorrelation is prominent when we look into the temporal evolution of the fluctuations of the magnitude of force contributions from protein and water. For the three systems, this is shown in Fig. 3.

In Fig. 3, short time trajectories are shown for the forces on the relevant bonds in the three proteins, as mentioned in the figure. The anticorrelation is apparent in all of these

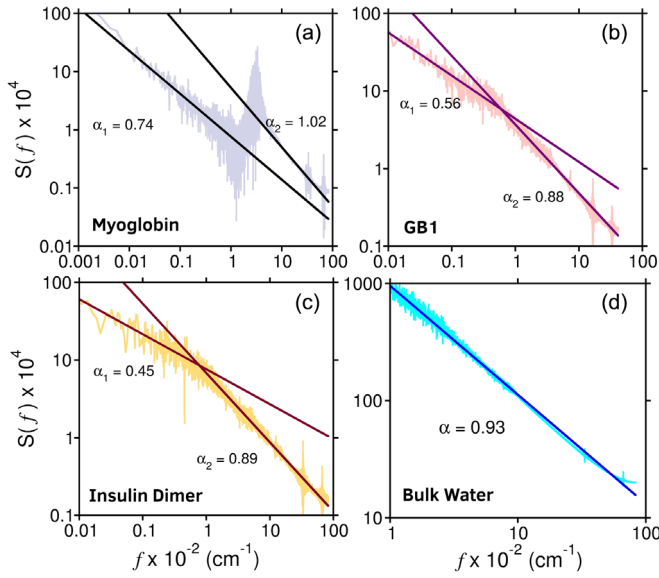


FIG. 4. Spectral density of the total force acting on the concerned bonds in the three proteins: (a) myoglobin, (b) GB1, and (c) insulin dimer. The spectra for all three systems show bimodal $1/f$ noise. The values of the slopes are given along the respective lines. The two distinct slopes originate because of coupling between protein and water fluctuations. The high frequency steeper slope (α_2) originates from water fluctuations [shown for neat water in (d)], while the low frequency one (α_1) is from protein, and depends on the nature of the protein.

trajectories. Some of them are highlighted by green rectangles. We observe a tug-of-war-like behavior between the contributions of force from protein and water.

We perform Fourier transformation of the FACF to get the spectral density of force. In Fig. 4 we plot this spectral density for the total force on the relevant bonds in all three systems (insulin dimer, GB1, and myoglobin, respectively). If the spectral density can be fitted to the form $S(f) \propto 1/f^\alpha$ (f = frequency), it is known as $1/f$ noise. Besides several natural phenomena, such noise has been reported for the fluctuations of protein and water as well [59,60]. In logarithmic representation, the slope of the linear curve provides the value of α . Interestingly, the total force spectrum exhibits bimodal $1/f$ noise characteristics, with the two slopes α_1 and α_2 .

The values of the slopes are given in Figs. 4(a)–4(c). We observe a general trend that $\alpha_1 < \alpha_2$. The value of α_2 shows a minimum deviation from protein to protein, with an average value around 0.9. The exponent α_1 , on the other hand, ranges from 0.45 to 0.74. To understand the origin of this bimodal $1/f$ noise, we calculate the force spectrum on a fixed water-water hydrogen bond in bulk water from a separate simulation. We find that this yields a spectrum with a single slope having a value of 0.93 [Fig. 4(d)]. Hence, the high frequency steeper slope in the protein systems (α_2) has its origin in the fluctuations of water. This arises from the low dielectric constant of the protein interior

that allows a strong interaction between the bonds and the water molecules. Since all of these bonds contain a certain degree of dipolar character, they may couple strongly to the polarization fluctuations of water. This is reflected in the exponent being close to unity in the $1/f$ noise of the force spectrum.

The slope at low frequency originates from the force contribution of the protein itself. It is sensitive to the nature of the protein. Hence it shows a large deviation from system to system.

In order to calculate frictional effects on rate, we need the frequency-dependent friction which is obtained by Laplace transformation of the FACF, which exhibits both a fast and a slow component. The fast component serves to reduce the total friction but populates the high frequency part of the power spectrum. The slow component enhances the zero frequency friction. To understand the effects of the frictional forces on the rates, we calculate the reaction rates based on three reaction rate theories, namely Kramers theory, Smoluchowski theory, and the more accurate Grote-Hynes theory [39]. The effects of the bimodality of frequency-dependent friction on the rate of a reaction can be addressed only via a non-Markovian rate theory like Grote-Hynes theory if we assume that the reaction surface is one dimensional. However, comparison between the three limits is instructive.

According to the Kramers theory, rate constant is given by Eq. (8).

$$k_{\text{Kr}} = \frac{1}{\omega_b} \left[\left(\frac{\zeta^2}{4} + \omega_b^2 \right)^{1/2} - \frac{\zeta}{2} \right] k_{\text{TST}}. \quad (8)$$

Here, ζ is the friction coefficient, ω_b denotes the frequency associated with the barrier, and k_{TST} is the transition theory rate constant. Here, we calculate the transmission coefficient defined as $\kappa = k/k_{\text{TST}}$, for all the three reaction systems studied [40]. In the overdamped limit (known as Smoluchowski limit), the transmission coefficient becomes ω_b/ζ . It is important to note that in Kramers' theory, we assume that the random forces are uncorrelated, and hence, friction is frequency independent.

According to the non-Markovian Grote-Hynes theory, the transmission coefficient is given by λ_r/ω_b where the reactive frequency λ_r is obtained by solving a self-consistent equation [Eq. (9)].

$$\lambda_r = \frac{\omega_b^2}{\lambda_r + \hat{\zeta}(\lambda_r)}. \quad (9)$$

$\hat{\zeta}(\lambda_r)$ denotes the frequency-dependent friction and is calculated by Laplace transformation of FACF. In the calculation of this quantity, we need both the frequency-dependent friction and the value of the barrier frequency. Here, we assume $\omega_b = 8 \text{ ps}^{-1}$. We vary this value between 5 and 12 ps^{-1} , and confirm that the basic conclusions do

not change. This range of barrier frequencies is expected in biochemical processes [39]. This also follows from our earlier work on insulin dimer dissociation [61].

In all the three cases, friction is found to reduce the value of the rate from the TST prediction significantly, revealing the dynamical effects of friction. Additionally, memory effects are found to play important role in determining the transmission coefficient. Because of the presence of the large ultrafast component in FACF, the reactions should be categorized in the intermediate damping regime. This is also borne out by the large difference in calculated rates between the Markovian and non-Markovian limits.

The negative contribution of the protein-water cross term can have an important consequence on the viscosity dependence of the rate of the bond-breaking processes in proteins. Here, the viscosity dependence will be determined by a competition between the following factors: (i) the barrier frequency, (ii) both the high and low frequency components of the total friction. These factors together determine the extent of damping of the reaction and hence the viscosity dependence of the rate. The cross term that is found to reduce the friction, both at high and low frequencies, could change with solvent's viscosity, in such a way that the high-frequency contribution decreases, which is reflected in the decrease of the rate. On the other hand, if the barrier frequency increases ($>10 \text{ ps}^{-1}$), the non-Markovian rate theory usually predicts weak viscosity dependence, since the slower solvent modes cannot couple to barrier crossing dynamics when driven at such a large frequency.

We surmise that the present calculation might serve to explain the experimental observation of weak viscosity dependence. In proteins it is often attributed to the dominant role of the internal friction. We offer a different scenario. Not only the negative cross-correlation between internal and external forces, but also the non-Markovian effects could play an important role in weakening the solvent viscosity dependence. This is akin to the breakdown of Kramers theory in isomerization reactions well known in literature [62,63]. If the Smoluchowski limit (SL) description were to be valid, we would expect a $1/\eta$ dependence of the reaction rate on viscosity (η). However, the inadequacy of the SL implies a weaker viscosity dependence, as was also observed earlier in the breakdown of Kramers theory [62,63].

We present the important result that the forces acting on these well-defined reaction coordinates derive contributions both from protein and water. These two exhibit pronounced anticorrelated fluctuations with time. The total friction on the bonds, calculated directly from the Kirkwood formula, thus derives a significant contribution from the cross-friction term between these two forces. We find that this cross term is negative and large, and significantly lowers the magnitude of the total friction, thereby acting as a lubricant that enhances the dissociation

rate. This protein-water coupling results in a bimodal $1/f$ noise in the force spectrum. The high frequency mode derives contribution from the forces exerted by water, while the relatively lower frequency mode originates from protein fluctuations, and is strongly dependent on the nature of the protein. These features are important in a non-Markovian rate theory, as discussed earlier.

We thank Professor S. Natarajan and Dr. S. Sarkar for constructive suggestions in this work. B. B. thanks Science and Engineering Research Board (SERB), India for support from the National Science Chair Professorship and Department of Science and Technology, India for partial research funding. S. Mu. and S. Mo. thank SERB, India and Indian Institute of Science (IISc) for support from the research fellowship. S. A. thanks IISc for support from the research fellowship. All the simulations were performed on the SahasraT Cray XC40 supercomputer at the Supercomputer Education and Research Centre, IISc.

*bbagchi@iisc.ac.in

- [1] P. Ball, *Life's Matrix: A Biography of Water* (University of California Press, Berkeley, 2001).
- [2] B. Bagchi, *Water in Biological and Chemical Processes: From Structure and Dynamics to Function* (Cambridge University Press, Cambridge, England, 2013).
- [3] L. D. Barron, L. Hecht, and G. Wilson, *Biochemistry* **36**, 13143 (1997).
- [4] D. De Sancho, A. Sirur, and R. B. Best, *Nat. Commun.* **5**, 4307 (2014).
- [5] W. Zheng, D. De Sancho, T. Hoppe, and R. B. Best, *J. Am. Chem. Soc.* **137**, 3283 (2015).
- [6] C. Päslock, L. V. Schäfer, and M. Heyden, *Phys. Chem. Chem. Phys.* **23**, 5665 (2021).
- [7] A. De Simone, C. Kitchen, A. H. Kwan, M. Sunde, C. M. Dobson, and D. Frenkel, *Proc. Natl. Acad. Sci. U.S.A.* **109**, 6951 (2012).
- [8] P. W. Fenimore, H. Frauenfelder, B. H. McMahon, and F. G. Parak, *Proc. Natl. Acad. Sci. U.S.A.* **99**, 16047 (2002).
- [9] H. Frauenfelder, G. Chen, J. Berendzen, P. W. Fenimore, H. Jansson, B. H. McMahon, I. R. Stroe, J. Swenson, and R. D. Young, *Proc. Natl. Acad. Sci. U.S.A.* **106**, 5129 (2009).
- [10] S. Mukherjee, S. Mondal, and B. Bagchi, *Phys. Rev. Lett.* **122**, 058101 (2019).
- [11] J. D. Bryngelson and P. G. Wolynes, *J. Phys. Chem.* **93**, 6902 (1989).
- [12] P. G. Wolynes, J. N. Onuchic, and D. Thirumalai, *Science* **267**, 1619 (1995).
- [13] D. Wales, *Energy Landscapes: Applications to Clusters, Biomolecules and Glasses* (Cambridge University Press, Cambridge, England, 2003).
- [14] J. J. Portman, S. Takada, and P. G. Wolynes, *J. Chem. Phys.* **114**, 5082 (2001).
- [15] R. B. Best and G. Hummer, *Phys. Rev. Lett.* **96**, 228104 (2006).

- [16] A. Ansari, C. M. Jones, E. R. Henry, J. Hofrichter, and W. A. Eaton, *Science* **256**, 1796 (1992).
- [17] D. Klimov and D. Thirumalai, *Phys. Rev. Lett.* **79**, 317 (1997).
- [18] A. Soranno, A. Holla, F. Dingfelder, D. Nettels, D. E. Makarov, and B. Schuler, *Proc. Natl. Acad. Sci. U.S.A.* **114**, E1833 (2017).
- [19] G. S. Jas, W. A. Eaton, and J. Hofrichter, *J. Phys. Chem. B* **105**, 261 (2001).
- [20] R. R. Cheng, A. T. Hawk, and D. E. Makarov, *J. Chem. Phys.* **138**, 074112 (2013).
- [21] T. Simonson and C. L. Brooks, *J. Am. Chem. Soc.* **118**, 8452 (1996).
- [22] D. W. Oxtoby, *J. Chem. Phys.* **70**, 2605 (1979).
- [23] D. W. Oxtoby and S. A. Rice, *Chem. Phys. Lett.* **42**, 1 (1976).
- [24] D. W. Oxtoby, *Adv. Chem. Phys.* **47**, 487 (1981).
- [25] D. W. Oxtoby, *Annu. Rev. Phys. Chem.* **32**, 77 (1981).
- [26] Yongnan D. Li, G. Lamour, J. Gsponer, P. Zheng, and H. Li, *Biophys. J.* **103**, 2361 (2012).
- [27] Z. Guo, H. Hong, G. Yuan, H. Qian, B. Li, Y. Cao, W. Wang, C.-X. Wu, and H. Chen, *Phys. Rev. Lett.* **125**, 198101 (2020).
- [28] K. Ding, J. M. Louis, and A. M. Gronenborn, *J. Mol. Biol.* **335**, 1299 (2004).
- [29] R. B. Best and J. Mittal, *Proteins* **79**, 1318 (2011).
- [30] S. Mondal, S. Mukherjee, S. Acharya, and B. Bagchi, *J. Phys. Chem. B* (2021).
- [31] P. Banerjee, S. Mondal, and B. Bagchi, *J. Chem. Phys.* **149**, 114902 (2018).
- [32] Z. Ganim, K. C. Jones, and A. Tokmakoff, *Phys. Chem. Chem. Phys.* **12**, 3579 (2010).
- [33] X.-X. Zhang, K. C. Jones, A. Fitzpatrick, C. S. Peng, C.-J. Feng, C. R. Baiz, and A. Tokmakoff, *J. Phys. Chem. B* **120**, 5134 (2016).
- [34] V. Zoete, M. Meuwly, and M. Karplus, *Proteins* **61**, 79 (2005).
- [35] S. Mukherjee, S. Acharya, S. Mondal, P. Banerjee, and B. Bagchi, *J. Phys. Chem. B* **125**, 11793 (2021).
- [36] R. Zwanzig, *Nonequilibrium Statistical Mechanics* (Oxford University Press, New York, 2001).
- [37] R. Kubo, *Rep. Prog. Phys.* **29**, 255 (1966).
- [38] J. G. Kirkwood, *J. Chem. Phys.* **14**, 180 (1946).
- [39] B. Bagchi, *Molecular Relaxation in Liquids* (Oxford University Press, New York, 2012).
- [40] See Supplemental Material at <http://link.aps.org/supplemental/10.1103/PhysRevLett.128.108101> for simulation methods, force autocorrelation functions, rate calculation, and internal friction from protein fluctuations, which includes Refs. [41–50].
- [41] D. Van Der Spoel, E. Lindahl, B. Hess, G. Groenhof, A. E. Mark, and H. J. Berendsen, *J. Comput. Chem.* **26**, 1701 (2005).
- [42] H. M. Berman, J. Westbrook, Z. Feng, G. Gilliland, T. N. Bhat, H. Weissig, I. N. Shindyalov, and P. E. Bourne, *Nucl. Acid Res.* **28**, 235 (2000).
- [43] C. Oostenbrink, A. Villa, A. E. Mark, and W. F. Van Gunsteren *J. Comput. Chem.* **25**, 1656 (2004).
- [44] H. Berendsen, J. Grigera, and T. Straatsma, *J. Phys. Chem.* **91**, 6269 (1987).
- [45] W. H. Press, H. William, S. A. Teukolsky, A. Saul, W. T. Vetterling, and B. P. Flannery, *Numerical Recipes*, 3rd ed., The Art of Scientific Computing (Cambridge University Press, Cambridge, England, 2007).
- [46] D. Frenkel and B. Smit *Understanding Molecular Simulation* (Elsevier, New York, 2002).
- [47] W. G. Hoover, *Phys. Rev. A* **31**, 1695 (1985).
- [48] M. Parrinello and A. Rahman, *J. App. Phys.* **52**, 7182 (1981).
- [49] T. Darden, D. York, and L. Pedersen, *J. Chem. Phys.* **98**, 10089 (1993).
- [50] B. Hess, H. Bekker, H. J. Berendsen, and J. G. Fraaije, *J. Comput. Chem.* **18**, 1463 (1997).
- [51] J. E. Straub, M. Borkovec, and B. Berne, *J. Phys. Chem.* **91**, 4995 (1987).
- [52] T. Li, M. L. Quillin, G. N. Phillips Jr, and J. S. Olson, *Biochem.* **33**, 1433 (1994).
- [53] R. Jimenez, G. R. Fleming, P. Kumar, and M. Maroncelli, *Nature (London)* **369**, 471 (1994).
- [54] S. Mondal, S. Mukherjee, and B. Bagchi, *Chem. Phys. Lett.* **683**, 29 (2017).
- [55] A. Soranno, B. Buchli, D. Nettels, R. R. Cheng, S. Muller-Spath, S. H. Pfeil, A. Hoffmann, E. A. Lipman, D. E. Makarov, and B. Schuler, *Proc. Natl. Acad. Sci. U.S.A.* **109**, 17800 (2012).
- [56] M. Berkowitz and W. Wan, *J. Chem. Phys.* **86**, 376 (1987).
- [57] P. G. Wolynes, *J. Chem. Phys.* **68**, 473 (1978).
- [58] B. Bagchi, *J. Chem. Phys.* **95**, 467 (1991).
- [59] I. Ohmine and H. Tanaka, *Chem. Rev.* **93**, 2545 (1993).
- [60] A. R. Bizzarri and S. Cannistraro, *Physica (Amsterdam)* **267A**, 257 (1999).
- [61] S. Acharya, S. Mondal, S. Mukherjee, and B. Bagchi, *J. Phys. Chem. B* **125**, 9678 (2021).
- [62] S. P. Velsko, D. H. Waldeck, and G. R. Fleming, *J. Chem. Phys.* **78**, 249 (1983).
- [63] B. Bagchi, *Int. Rev. Phys. Chem.* **6**, 1 (1987).